Numerical simulation of formation optimization for a fleet of unmanned surface vehicles based on a minimum energy consumption requirement

Zhenpeng Dong*, and *Xiao* Liang

School of Naval Architecture and Ocean Engineering, Dalian Maritime University, Dalian, Liaoning Province, People's Republic of China

Abstract. This study proposes a hydrodynamic optimization strategy focusing on minimum energy consumption to construct the formation of a fleet of unmanned surface vehicles (USVs) by transforming the longitudinal offset and transverse separation. USVs were used instead of Autonomous Underwater Vehicles (AUVs) to fully consider the influence of a wave on energy-savings and to address undersize spacing and limited wake. The numerical model provided reasonably accurate results when compared against a series of experimental prototype results. The body force model was used to replicate the impact of the propeller, and an echelon formation was arranged considering the aft wedge wave pattern region induced by the Kelvin wave. The energy consumption equations of two-, three-, and four-hull formations were denoted by resistance components and used to determine the energy relationship between individuals and collectives. Additionally, an optimization platform was developed to integrate the application programs because the computation times were extensive for numerical simulations of spacing configurations transformation

1 Introduction

Unmanned surface vehicles (USVs) become a new generation of robots that obtain self-propelled performance and have the capability to perform missions without requiring external powering or control. One of most important advantages of USV is that the activity range obtains a significant expansion by changing the operation environment from underwater to surface when compared with the Autonomous Underwater Vehicles (AUVs). Traditional single-hull navigation mode is difficult to execute the complex water-surface tasks. It is necessary to construct formation for a fleet of USVs to overcome the limitations in endurance and energy consumption of the single-hull mode [1-3].

Observations from animal behavior such as schooling fish maintain their tailbeat [4], dolphin cub swims close to mother's abdomen [5], wild geese fly in an echelon formation [6], and duckling rides wave behind its mother [7] reflect the energy-saving phenomenon induced by moving near neighbours. The concept of formation energy-saving have begun to

* Corresponding author: dongzhenpeng@126.com

emerge that can apply to a vessel fleet. Previous studies indicated that the energy benefit depends on the hydrodynamic behavior of the fleet [8-11]. Therefore, the spacing distance between the hulls is a primary formation consideration, which provides a wave flow to transfer the energy from the leader to the follower.

There are two groups of spacing configurations: the transverse separation and longitudinal offset. The transverse separation strives to distance the hull from other vehicles from the perspective of safety, which is related to the transverse distance between the centerlines of each body. The longitudinal offset restricts the team order depending on the operators to determine the leader and follower. This corresponds to the longitudinal distance between the nose of each body.

This study proposes a hydrodynamic optimization strategy focusing on minimum energy consumption to construct the formation of a fleet of USVs by transforming the longitudinal offset and transverse separation. USVs were used instead of AUVs to fully consider the influence of a wave on energy-savings and to address undersize spacing and limited wake. The hydrodynamic mechanism of formation energy-saving was revealed by analyzing the variation of the resistance.

2 Numerical method

The upstream flow of the follower comes from the downstream flow of the leader. Therefore, the follower receives a combined wave which is composed of two parts: the free inflow from the water, and the propeller race from the leader. The leader only receives a steady inflow without fluid-structure interaction. The combined wave exists in water channel among the members. The propeller propulsion of the leader pushes it backward to the follower, leading to the propeller excitation. As a result, the follower obtains a re-energized flow to ameliorate the surrounding flow field.

The energy-savings of the fleet depend on the wake expansion induced by the propeller. The propeller motion accelerates the wake to derive the Kelvin wave region. Hough and Ordway [12] proposed a RANS-HO body force model to calculate the axial and tangential momentum source terms by using a virtual disc to replicate the impact of a real propeller. These two momentum source terms were applied to the radial direction of the propeller, and the thrust and torque were generated subject to the circulation distribution.

The body force model was used in Reynolds Averaged Navier Stokes (RANS) simulations [13] to become the RANS-HO method. By assuming the thrust and torque distributions are independent, Fb_x and Fb_θ can be respectively expressed as:

$$\mathrm{Fb_x} = \mathrm{A_x r^*}(1 - \mathrm{r^*})^{1/2} \tag{1}$$

$$\mathrm{Fb_\theta} = \mathrm{A_\theta r^*}(1 - \mathrm{r^*})^{1/2} / (\mathrm{r^*} - \mathrm{r^* Y_h} + \mathrm{Y_h}) \tag{2}$$

where Fb_x and Fb_θ are the non-dimensional thrust and torque distributions, respectively. r^* is the non-dimensional radius calculated by $(Y - Y_h) / (1 - Y_h)$, and Y and Y_h can be respectively written as:

$$Y = r_p / R_p \tag{3}$$

$$Y_h = R_h / R_p \tag{4}$$

where R_p and R_h are the radius of the propeller and the hub, respectively. r_p is the straight-line distance from an arbitrary point in the virtual disc region to the propeller axial line.

Note that A_x and A_θ can be respectively written as:

$$A_x = 105K_T / [16\Delta x(4 + 3Y_h)(1 - Y_h)] \quad (5)$$

$$A_\theta = 105K_Q / [\pi\Delta x J^2(4 + 3Y_h)(1 - Y_h)] \quad (6)$$

where K_T and K_Q are the thrust coefficient and torque coefficient, respectively. Δx is the thickness of the propeller hub, and is given by user. J is the propeller advance coefficient. Moreover, K_T and K_Q can be respectively expressed as:

$$K_T = T / (\rho n^2 D^4) \quad (7)$$

$$K_Q = Q / (\rho n^2 D^5) \quad (8)$$

where T and Q are the thrust and torque, respectively. ρ is the density of water. n is the revolutions per second. D is the propeller diameter.

3 Validation

A series of prototype experiments were conducted in the open water tank, as shown in Fig. 1. The single-hull validation was performed at first, and then expanded to the formation construction of the fleets. The tested USV was self-developed by the Dalian Maritime University Unmanned System Technical Team, and was equipped with the propeller to supply the self-propulsion performance in waves. The main particulars are listed in Table 1.

Fig. 1. Prototype modelling and water tank test.

Table 1. Dimensions of the USV parameters.

Parameters	Unit	Dimension
Length	m	1.25
Beam	m	0.35
Draft	m	0.14
Displacement	m^3	0.0477
Speed	m / s	1 ~ 3
Propeller diameter	m	0.1
Propeller thickness	m	0.02
Number of blades		4
Propeller center		(0.58, 0, -0.05)

The hydrodynamic and movement characteristics of the USV can be obtained from the prototype test. The precision validation was discussed in terms of the total resistance and

heave, as shown in Fig. 2. The numerical simulation results were in good agreement with the physical experiment results. The numerical model was proved to apply in the follow-up formation simulations composed of multiple USVs.

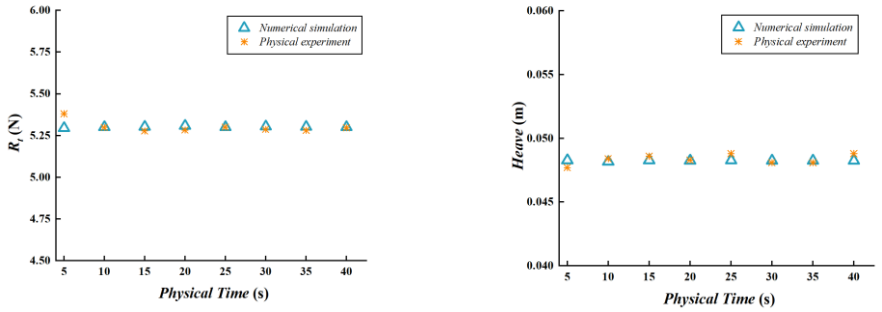

Fig. 2. Precision validation.

4 Formation configurations

The follower needs to be placed behind the leader to construct the formations. To be exact, the trailing USV was positioned at the Kelvin wave region excited by the leader USV where the most intense hydrodynamic interaction occurred. Therefore, the possibility of energy-saving for the fleet may be improved by using the echelon formation.

4.1 Echelon formation construction

Two spacing configurations including the transverse separations (S / L) and longitudinal offsets (D / L) were defined by considering the Kelvin wave influences, the minimum safe distance, and the maximum communication distance. The transverse separation is related to the transverse distance between the centerlines of each body. The longitudinal offset is related to the longitudinal distance between the nose of each body. The formation geometry was transformed freely by switching the spacing configurations. The member's quantity was extended from two to four to construct a relatively complex formation as much as possible by considering the Kelvin wave expansion, as shown in Fig. 3.

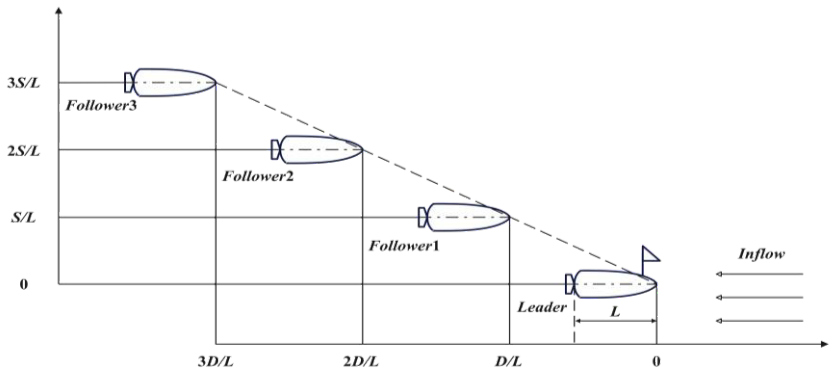

Fig. 3. Echelon formation construction based on two spacing configurations.

4.2 Formation energy consumption

The energy consumption index was denoted as the percentage difference in terms of the resistance. The energy relationship between individuals and collectives was determined by using the uniform magnitude of the energy consumption index.

The follow-up formation transformation referenced to the initial formation configuration. The energy consumption index in the two-hull formation can be expressed as:

$$\begin{aligned} \%A &= (R_{A_1} - R_A) / R_A \times 100 \\ \%B &= (R_{B_1} - R_B) / R_B \times 100 \\ \%EC &= [(R_{A_1} + R_{B_1}) - (R_A + R_B)] / (R_A + R_B) \times 100 \end{aligned} \tag{9}$$

where R_{A_1} and R_{B_1} are the individual resistances of the leader USV A_1 and follower USV B_1 in the follow-up formation case, respectively. R_A and R_B are the individual resistances of the leader and follower in the initial formation case, respectively. $\%A$, $\%B$, and $\%EC$ are the energy consumption indexes with percentage difference forms for the single leader-hull, single follower-hull, and the whole fleet, respectively.

The energy consumption index in the three-hull formation should consider another set of spacing configurations because the second follower B_2 was added in the fleet. This is expressed as:

$$\begin{aligned} \%A &= (R_{A_1} - R_A) / R_A \times 100 \\ \%B &= (R_{B_1} - R_B) / R_B \times 100 \\ \%C &= (R_{C_1} - R_C) / R_C \times 100 \\ \%EC &= [(R_{A_1} + R_{B_1} + R_{C_1}) - (R_A + R_B + R_C)] / (R_A + R_B + R_C) \times 100 \end{aligned} \tag{10}$$

where R_{C_1} and R_C are the individual resistances of the second follower in the follow-up formation case and initial formation case, respectively. $\%C$ and $\%EC$ are the individual energy consumption for the single hull of B_2 and total energy consumption for the fleet, respectively.

Likewise, when the third follower B_3 was added in the fleet, a new group of spacing configurations were considered in a four-hull formation, and the energy consumption index is changed as:

$$\begin{aligned} \%A &= (R_{A_1} - R_A) / R_A \times 100 \\ \%B &= (R_{B_1} - R_B) / R_B \times 100 \\ \%C &= (R_{C_1} - R_C) / R_C \times 100 \\ \%D &= (R_{D_1} - R_D) / R_D \times 100 \\ \%EC &= [(R_{A_1} + R_{B_1} + R_{C_1} + R_{D_1}) - (R_A + R_B + R_C + R_D)] / (R_A + R_B + R_C + R_D) \times 100 \end{aligned} \tag{11}$$

where $\%D$ is the individual energy consumption for the single hull of B_3. $\%EC$ is the total energy consumption referenced to the sum of all USVs' resistances.

Note that the energy consumption index has the positive and negative properties by using the "-" and "+" signs. The "-" sign represents an energy-saving with a positive benefit, the "+" sign represents an energy deficit with a negative benefit.

4.3 Formation optimization circulation

The formation shape was reconstructed by switching the spacing configurations. One simulation execution was corresponding to one parameter assignment of the spacing configuration, leading to huge amount of computational cost. In order to achieve the automatic switching process, the simulations were integrated in an optimization platform that can apply to implement multiple software interaction.

The integrated circulation was designed as two layers nest mode. The optimal algorithms were provided in the outer layer to create the experimental matrix, while the simulations were executed in the inner layer. Different modules were serially integrated to extend the circulation flow function including function mapping, data exchange, geometric modelling, read-in and write-out, simulation, file clean-up, and data storage. Finally, the inner and outer layer were encapsulated to derive a complete closed circulation flow, as shown in Fig. 4. When one circulation ends, the next circulation will automatically run. The optimization is not completed until all circulation flows are executed.

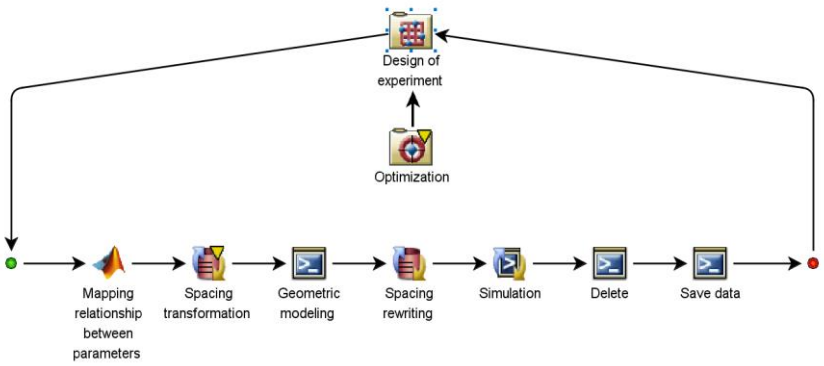

Fig. 4. Integrated circulation to automatically optimize the formation.

5 Results

The two-, three-, and four-hull formations were optimized by switching the spacing configurations with transverse separation and longitudinal offset. Some configurations existed in the optimization process that had a significant energy benefit for the entire fleet. However, some configurations led to the adverse result of an energy burden for the fleet. To be exact, when compared with the initial formation, the optimal formation arranged the vehicles in a beneficial region to obtain the profitable wave flow, and then the energy consumptions of the individuals and fleet were decreased. The worst formation experienced the unprofitable wave superpositions or the propeller propulsion interferences, leading to the increment of the energy consumption. The formation results are presented in Fig. 5.

Some findings of the simulations showed that the optimal formation existed, whether for two-, three-, and four-hull formations, which can obtain the minimum energy consumption for individuals and the entire fleet. The energy consumption saving efficiency decreased when the number of members increased, as depicted in Fig. 6. This is because the

wave occurred the multiple superpositions. Moreover, the range of the beneficial region corresponding to the optimal spacing configurations was further compressed due to the energy-savings for a fleet became more difficult.

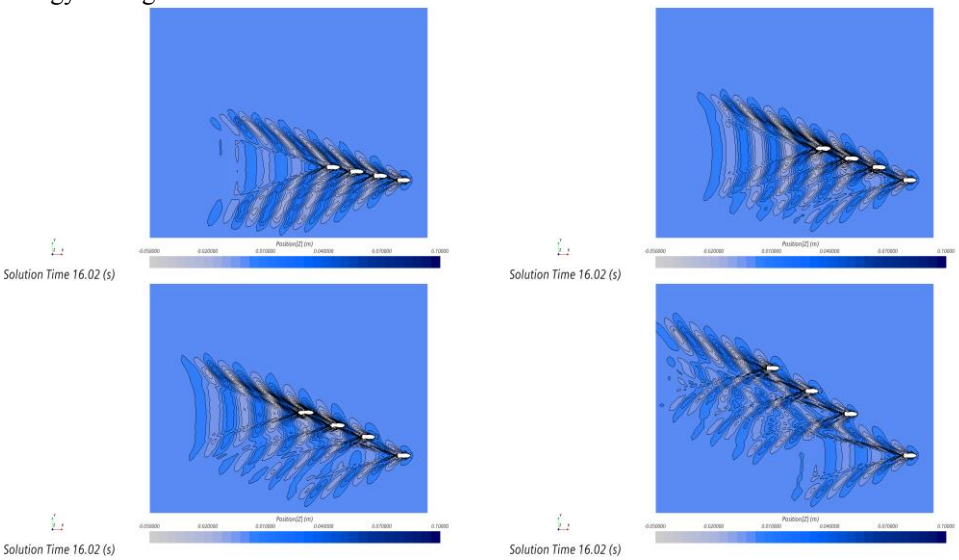

Fig. 5. Formation wave pattern. According to clockwise direction: the initial, worst, normal, and optimal formation.

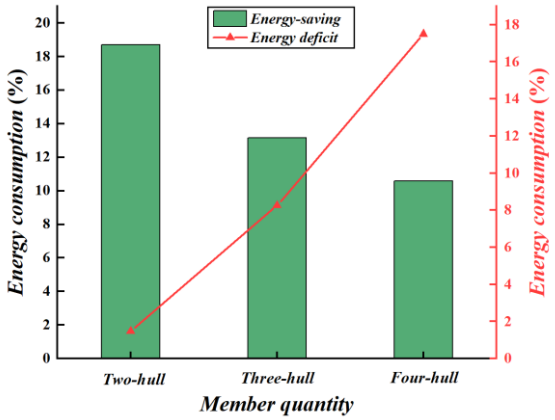

Fig. 6. Minimum energy consumptions for two-, three-, and four-hull formations.

References

1. Z. P. Dong, X. Liang, Y. H. Hou, Z. Zhang, Ocean. Eng, **249** (2022)
2. X. Liang, Z. P. Dong, Y. H. Hou, X. Y. Mu, Ocean. Eng, **218** (2020)
3. A. F. Molland, I. K. A. P. Utama, Proc. Inst. Mech. Eng, Part M: J Eng. Marit. Environ, **216**, 107-117 (2002)
4. L. Li, M. Nagy, J. M. Graving, J. Bak-Coleman, G. M. Xie, I. D. Couzin, Nat Commun, **11** (2020).
5. D. Weihs, J. Biol, **3**, 1-16 (2004)

6. M. Andersson, J. Wallander, Behav. Ecol, **15**, 158-162 (2003)
7. Z. M. Yuan, M. L. Chen, L. B. Jia, C. Y. Ji, A. Incecik, J. Fluid Mech, **928** (2021)
8. A. B. Phillips, S. R. Turnock, M. Furlong, Ship Technol. Res, **57**, 128-139 (2010)
9. A. B. Phillips, S. R. Turnock, M. Furlong, J. Mar. Sci. Technol, **15**, 201-217 (2010)
10. P. Rattanasiri, P. A. Wilson, A. B. Phillips, Indian J. Mar. Sci, **42**, 964-970 (2013)
11. P. Rattanasiri, P. A. Wilson, A. B. Phillips, Ocean. Eng, **80**, 25-35 (2014)
12. G. Hough, D. Ordway, Dev. Theor. Appl. Mech, **2**, 317-336 (1965)
13. P. Rattanasiri, P. A. Wilson, A. B. Phillips, Ocean. Eng, **100**, 126-137 (2015)